8-18-2017

Intrinsic Hydrophobicity versus Intraguest Interactions in Hydrophobically Driven Molecular Recognition in Water

Roshan W. Gunasekara
Iowa State University

Yan Zhao
Iowa State University, zhaoy@iastate.edu

Intrinsic Hydrophobicity versus Intraguest Interactions in Hydrophobically Driven Molecular Recognition in Water

Abstract

Molecular recognition of water-soluble molecules is challenging but can be achieved if the receptor possesses a hydrophobic binding interface complementary to the guest. When the guest molecule contains more than one hydrophobic group, intrahost interactions between the hydrophobes could strongly influence the binding of the guest by its host. In a series of ornithine derivatives functionalized with aromatic hydrophobes, the most electron-rich compound displayed the strongest binding, despite its lowest intrinsic hydrophobicity.

Disciplines

Organic Chemistry

Intrinsic Hydrophobicity versus Intraguest Interactions in Hydrophobically Driven Molecular Recognition in Water

Roshan W. Gunasekara and Yan Zhao*

Department of Chemistry, Iowa State University, Ames, Iowa 50011-3111

Supporting Information Placeholder

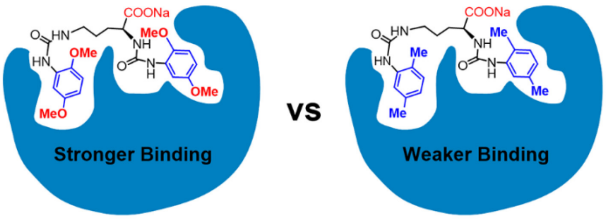

ABSTRACT: Molecular recognition of water-soluble molecules is challenging but can be achieved if the receptor possesses a hydrophobic binding interface complementary to the guest. When the guest molecule contains more than one hydrophobic group, intrahost interactions between the hydrophobes could strongly influence the binding of the guest by its host. In a series of ornithine derivatives functionalized with aromatic hydrophobes, the most electron-rich compound displayed the strongest binding, despite its lowest intrinsic hydrophobicity.

Molecular recognition in water is an important and yet challenging topic in supramolecular chemistry.[1] Many hydrophobic molecules including peptides have multiple hydrophobes in the structure, often scattered along a backbone with its own conformational preferences. In such cases, hydrophobically based molecular recognition needs to take into account not only the interactions between the host and the guest but also those within the host or guest.[2] We recently reported a class of multifunctional cross-linked micelles as highly specific peptide receptors in water.[3] Binding selectivity was achieved by the "hydrophobic dimples" created on the surface of the micelles complementary to the hydrophobic side chains of the peptides. In this work, we seek to understand what other factors might affect the binding strength for water-soluble guest molecules, in addition to the host–guest complementarity.[4]

The receptors in this study were created through micellar molecular imprinting, a method recently developed in our laboratory (Scheme 1).[5] The method involves surface-cross-linking of the micelle of **1** by click reaction using diazide **2**. The micelle normally contains an equivalent amount of divinylbenzene (DVB), a small amount of a photoinitiator (DMPA), and a template molecule. The surface-cross-linked micelle (SCM) is functionalized with ligand **3** to enhance its solubility in water and facilitate its recovery and purification. The ligand also enables the cross-linked micelles to be soluble in organic solvents such as DSMO but insoluble in less hydrogen-bonding solvents such as ethyl acetate or acetone. Free radical polymerization, initiated by UV irradiation, cross-links the core around the template, forming the complementary binding pocket in the meantime. The resulting molecularly imprinted nanoparticles (MINPs) have been shown to recognize a number of water-soluble molecules including bile salt derivatives,[5] nonsteroidal anti-inflammatory drugs (NSAIDs),[6] and carbohydrates if appropriate binding functionalities are used.[7]

In this work, we chose to study template/guest molecules **4**–**9**. They all contain one or two hydrophobic groups and an ionic carboxylate to make the molecule soluble in water. The carboxylate also helps the incorporation of the compound into the cationic micelle of **1**, helpful to both the imprinting and the binding process. Compounds **4**–**7** contain two hydrophobes linked by a flexible ornithine-based tether, whereas **8** and **9** only one. The aromatic groups are substituted with methoxy, methyl, or nitro groups, changing the hydrophobicity of the ring and also their the electron density.

Scheme 1. Preparation of MINP by surface–core double cross-linking of template-containing micelle of **1**.

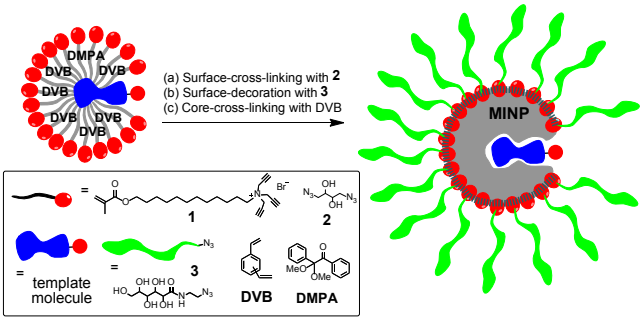

Table 1. Binding data for MINPs obtained by ITC.[a]

entry	host	guest	K_a ($\times 10^4$ M^{-1})	K_{rel}	ΔG (kcal/mol)	ΔH (kcal/mol)	$T\Delta S$ (kcal/mol)	N
1	MINP(**4**)	**4**	19.6 ± 1.1	1	-7.21	-11.83 ± 1.17	-4.62	0.8 ± 0.1
2	MINP(**4**)	**5**	6.11 ± 0.51	0.31	-6.52	-2.21 ± 0.25	4.31	1.1 ± 0.1
3	MINP(**4**)	**6**	2.94 ± 0.80	0.15	-6.09	-1.10 ± 0.69	4.99	1.2 ± 0.1
4	MINP(**4**)	**7**	0.49 ± 0.02	0.02	-5.03	-1.17 ± 0.34	3.86	1.2 ± 0.1
5	MINP(**5**)	**5**	7.11 ± 0.13	1	-6.61	-2.03 ± 0.87	4.59	0.9 ± 0.1
6	MINP(**5**)	**4**	4.08 ± 0.22	0.57	-6.28	-2.35 ± 0.20	3.93	0.9 ± 0.1
7	MINP(**5**)	**6**	1.84 ± 0.47	0.26	-5.82	-1.19 ± 0.09	4.63	1.1 ± 0.2
8	MINP(**5**)	**7**	0.83 ± 0.02	0.12	-5.34	-1.05 ± 0.08	4.29	1.1 ± 0.1
9	MINP(**6**)	**6**	6.50 ± 0.46	--	-6.56	-1.15 ± 0.12	5.41	1.1 ± 0.1
10	MINP(**7**)	**7**	1.90 ± 0.68	--	-5.83	-1.19 ± 0.50	4.64	0.9 ± 0.1
11	MINP(**8**)	**8**	0.53 ± 0.03	--	-5.08	-1.45 ± 1.06	3.63	0.8 ± 0.1
12	MINP(**9**)	**9**	0.92 ± 0.09	--	-5.40	-1.41 ± 0.50	3.99	0.9 ± 0.1

[a] The titrations were performed in duplicates in Millipore water and the errors between the runs were <10%. Our recent studies show that binding affinities for similar compounds were very similar in water and in 10 mM HEPES buffer at pH 7.4 (ref 3).

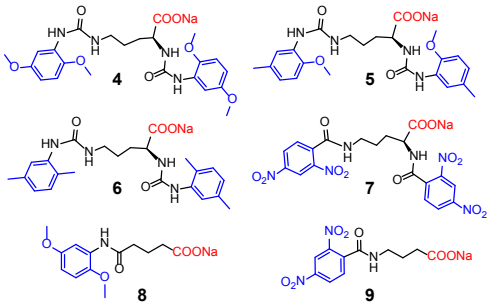

We synthesized and characterized the MINPs following previously reported procedures (see supporting information for details).[3, 5-6, 8] We studied their molecular-recognition properties by isothermal titration calorimetry (ITC).[9] To ensure that molecular imprinting worked well and highly guest-complementary receptors can be created for the current compounds, we first examined the binding of selected MINPs by different guest molecules. The indicator for successful imprinting would be strong and selective binding for the template molecules in comparison to their structural analogues.

According to Table 1, MINP(**4**), i.e., MINP prepared using molecule **4** as the template, bound the template with $K_a = 19.6 \times 10^4$ M^{-1} (entry 1). Compounds **5** and **6** differ only slightly from **4**, substituting one and two of the methoxy groups on the phenyl with methyl. Yet, MINP(**4**) was able to distinguish the compounds quite well. As shown by the relative binding constant (K_{rel}), i.e., the binding constant of the guest relative to that of the template, **5** and **6** were bound by MINP(**4**) with only 31% and 15% of the affinity for the template, respectively.

Compound **7** differs from **4**–**6** in the substitution pattern and the electron density of the phenyl ring. The nitro group also differs substantially from methyl or methoxy in size and shape. The K_{rel} value was only 0.02, indicating that the compound was bound by MINP(**4**) much more weakly in comparison to the other guests, highlighting the selectivity of our imprinted receptor.

We also performed a similar study with MINP(**5**). The strongest guest was again the template itself (**5**) and the nitro derivative (**7**) was bound the least, while **4** was bound slightly better than **6**. The binding selectivity thus has a similar trend as that of MINP(**4**), suggesting the most difficult-to-distinguish pair was **4** and **5**, with **6** and **7** being increasingly easier.

We only studied MINP(**4**) and MINP(**5**) in binding selectivity because our micellar imprinting has been confirmed by multiple previous studies to afford highly selective receptors,[5-7] even to the point of distinguishing the position of a single methyl group in leucine and isoleucine,[3] and the inversion of a single hydroxyl in mono- and oligosaccharides.[7] Having confirmed the effectiveness of the imprinting with MINP(**4**) and MINP(**5**), we began to study the binding between *different* MINPs and their *corresponding templates*, trying to identify the factors that control the binding affinity for the matched host–guest pairs.

Binding between typical MINPs and their guests in water are hydrophobically driven, reinforced by the electrostatic interactions between the cationic cross-linked micelle and negatively charged carboxylate.[5] A commonly used indicator for the hydrophobicity of a compound is the octanol/water partition coefficient, $P = \log K_{OW}$.[10] Since compounds **4**–**6** only differ in the aromatic hydrophobes, the P values[11] of *p*-dimethoxybenzene (2.03), *p*-methylanisole (2.66), and *p*-xylene (3.15) suggest that the hydrophobic driving force for compounds **4**–**6** to enter a complementary hydrophobic binding site should follow the order of **4** < **5** < **6**. The trend is reasonable given that a methoxy can hydrogen-bond with water molecules more easily than a methyl group. When the binding constants of these compounds with their corresponding MINPs were compared, however, a completely opposite order was observed, i.e., **4** > **5** > **6** (entries 1, 5, and 9).

The binding of **7** (entry 10) by its MINP was weaker than those of **4**–**6** (by their corresponding MINPs). However, because the aromatic hydrophobe of **7** differs from those of **4**–**6** in multiple aspects, including substitution pattern, electronic (deficient) nature, and the linkage (amide versus urea) to the ornithine, we may not be able to simply say the compound has a lower hydrophobic driving force in binding by the low P value of *m*-dinitrobenzene (1.49).

We then studied the binding of the single-hydrophobed compounds **8** and **9**, again by their own MINPs (entry 11 and 12). Only the dimethoxy- and dinitro-versions were studied because they represented the strongest and weakest guests in **4**–**7**. In these two compounds, we tried to keep the structures as similar as possible other than the hydrophobe—e.g., an amide linkage was used in both compounds, albeit connected to the phenyl ring in opposite directions (due to availability of the starting materials). Interestingly, the binding order was reversed, with the dinitro-derived **9** showing nearly twice as strong a binding than the

dimethoxy-derived **8**. Notable also is that doubling the number of the hydrophobe (i.e., the main molecular recognition unit for hydrophobic binding) essentially doubled the binding constant of the electron-deficient **9** (compare entries 12 and 10) but enhanced the binding of the electron-rich **8** by 37 times (compare entries 11 and 1).

Because the single- and double-hydrophobed compounds displayed different trends in the binding, a fundamental difference must exist between the two types of guest molecules. Also, what is common between the two types of guests cannot be used to explain the different binding trends. For the double-hydrophobed guests (**4**–**7**), the binding affinity clearly did *not* follow the side-chain hydrophobicity, even for the homologous **4**–**6** whose structural variation was tightly controlled. The result appears surprising for bindings driven by hydrophobic interactions (in addition to the electrostatic interactions between the micelle and the carboxylate, which should be constant within the series). Nevertheless, when all the double-hydrophobed guests (**4**–**7**) are considered together, their binding affinity seemed to correlate directly with the electron-density of the phenyl group, with **4** being the most electron-rich and **7** the most electron-deficient.

Aromatic interactions are known to have a number of contributions including electrostatic, van der Waals, and solvophobic interactions, with the solvophobic interactions dominating in polar solvents.[12] The interacting partners can adopt several geometries—i.e., edge-to-face, offset stacked, or face-to-face stacked—depending on the electronic nature of the aromatic systems and the media involved.[13] In general, the edge-to-face geometry is preferred by electron-rich aromatics to avoid strong repulsion of the aromatic π clouds.[14] Electron-deficient rings, however, tend to adopt offset stacked configuration so that the heteroatoms high in electron density can interact with the electron-deficient core of the aromatic ring.[15]

Our binding data are consistent with these geometries, which give the electron-rich compounds (**4**–**6**) a larger solvent-exposed surface area than the electron-deficient **7**. Not only so, from the binding trend displayed by **4**–**6**, the electron-richer the aromatic ring, the larger the water-exposed surface the compound has. As a result, the least hydrophobic compound (**4**) ended up being bound most strongly by its MINP—a peculiar and yet logical feature of hydrophobic binding of these guests with more than one aromatic rings.

It should be mentioned that our ITC data showed that the binding of **4** by MINP(**4**) was enthalpically driven and entropically unfavorable (entry 1), whereas all the other bindings had favorable enthalpic and entropic terms (Table 1). It is not clear to us what the exact cause was for the difference, as these bindings had multiple contributions including solvent effects. Nonetheless, the unique negative/unfavorable entropy in the binding of **4** suggests a less ordered ground state relative to its host–guest complex. Bearing three electron-donating groups, the aromatic rings in this compound is highly rich in electron density. It is possible that the repulsion between the electron-rich phenyls made the hydrophobic interactions between the two quite difficult, resulting in a less ordered conformation prior to binding.[16] On the other hand, strong solvophobic interactions between the aromatic rings only serve to collapse the structure, reducing the conformational freedom of the guest prior to binding.

Figure 1a shows the solutions of compounds **8**, **4**, **9**, and **7** in water, all at 1.0 mM concentration. With the electron-rich *p*-dimethoxyphenyl ring, **8** and **4** were both colorless and showed no difference. With the electron-deficient *m*-dinitrophenyl, the double-hydrophobed **7** showed significant more intense color than the single-hydrophobed **9**, indicative of substantial intramolecular interactions between the aromatics in the former.

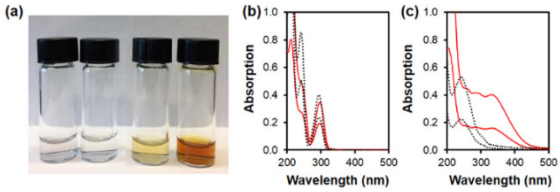

Figure 1. Solutions of compounds **8**, **4**, **9**, and **7** (from left to right) at 1.0 mM in water (a). UV-vis spectra of compounds (b) **4** (red solid line) and **8** (black dotted line) and (c) **7** (red solid line) and **9** (black dotted line) at 45 and 90 mM in water.

The color change above is reasonable from the point of binding geometry: with the electron-deficient dinitrophenyl rings in **7** adopting the offset stacked geometry, the π clouds are expected to be close in space and strongly perturb each other. Meanwhile, the face-to-face overlap between the off-stacked aromatics reduces the solvent-exposed surface area and, in turn, the hydrophobic driving force for **7** to enter its hydrophobic binding site.

For the electron-rich aromatics, the edge-to-face geometry separates the π clouds by a significant distance. Not only are the π clouds expected to be less perturbed, the smaller overalp of the aromatic rings also increases the sovlent-exposed surface area and, in turn, the hydrophobic binding force. In other words, poorly overlapped diaromatic guests should benefit more from the second aromatic ring in their hydrophobic binding than strongly overlapped ones, whose intramolecular hydrophobic interactions lowered the driving force for binding before binding occurs. This was indeed confirmed by the 37-fold enhancement in K_a from **8** to **4**, in contrast to the 2-fold increase from **9** to **7**.

Figure 1b,c shows the UV-vis spectra of these compounds, each at two different concentrations. According to Figure 1b, although the electron-rich pairs have subtly different absorption peaks, the two UV spectra are overall quite similar. The π system in **8**, therefore, is not perturbed too much as compared to those in **4**. For the electron-deficient pairs, however, a broad absorption in **7** in the range of 250 to >400 nm appeared that were absent in **9**, consistent with strong interactions of the π systems of the former. The π–π interactions were intramolecular in nature, as shown by the 2-fold enhancement in absorption of **7** when the concentration doubled.

^{1}H NMR spectroscopy showed similar results (Figure 2): whereas the aromatic protons of **4** showed only small upfield shifts compared to the single-hydrophobed **8** and remained well-resolved, the aromatic protons of **7** shifted strongly and became poorly resolved in comparison to **9**. The overall much larger upfield shifts in **7** is consistent with the off-stacked configuration of the aromatics. Note that intermolecular aggregation was already ruled out at much higher concentrations by the UV-vis spectroscopy (Figure 1b).

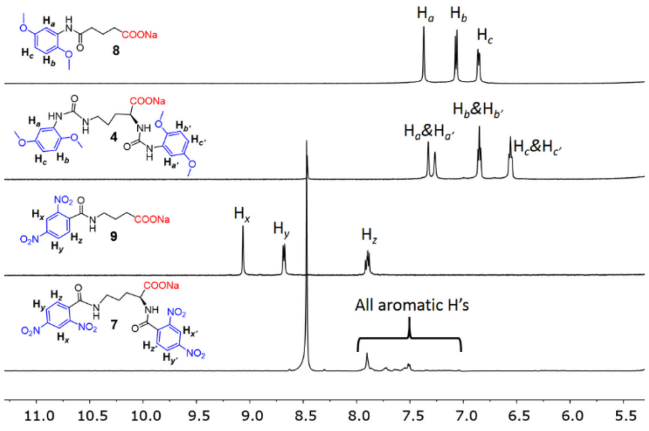

Figure 2. Portions of ^{1}NMR spectra of compounds **8**, **4**, **9**, and **7** at 1.2 mM in D_2O.

When more than one hydrophobe exists within the guest molecule, the *intraguest* hydrophobic interactions could have a strong impact on how the guest is bound by its host. Even when the host–guest interaction is largely hydrophobic in nature, our work shows that the *intraguest* interactions could change the hydrophobic driving force strongly to override the effect of intrinsic hydrophobicity. As a result, the most hydrophobic guest may not bind most strongly in water and could even become the weakest binder as shown by our binding data. For the same reason, the binding affinity of multi-hydrophobed compounds could not simply be extrapolated from that of the single-hydrophobed ones, as the intraguest interactions may differ from case to case. These phenomena are not expected to be limited to aromatic hydrophobes whose interactions have strong geometrical preferences. It is possible that, when the hydrophobes are scattered on a semirigid backbone (e.g., peptide), the *intraguest* interactions face constraints set by the covalent framework and could also influence their hydrophobic binding.

ASSOCIATED CONTENT

Supporting Information

Experimental details, ITC titration curves, and NMR data of key compounds (PDF).

AUTHOR INFORMATION

Corresponding Author

* E-mail: zhaoy@iastate.edu

ACKNOWLEDGMENT

We thank the NSF (CHE-1708526 and DMR-1464927) for financial support of this research.

REFERENCES

(1) (a) Oshovsky, G. V.; Reinhoudt, D. N.; Verboom, W., *Angew. Chem. Int. Ed.* **2007,** *46*, 2366-2393. (b) Kataev, E. A.; Müller, C., *Tetrahedron* **2014,** *70*, 137-167.
(2) (a) Gunasekara, R. W.; Zhao, Y., *J. Am. Chem. Soc.* **2015,** *137*, 843-849. (b) Gunasekara, R. W.; Zhao, Y., *Chem. Commun.* **2016,** *52*, 4345-4348.
(3) Awino, J. K.; Gunasekara, R. W.; Zhao, Y., *J. Am. Chem. Soc.* **2017,** *139*, 2188-2191.
(4) (a) Dougherty, D. A., *Science* **1996,** *271*, 163-168. (b) Rekharsky, M.; Inoue, Y.; Tobey, S.; Metzger, A.; Anslyn, E., *J. Am. Chem. Soc.* **2002,** *124*, 14959-14967. (c) Thompson, S. E.; Smithrud, D. B., *J. Am. Chem. Soc.* **2002,** *124*, 442-449. (d) Fiedler, D.; Leung, D. H.; Bergman, R. G.; Raymond, K. N., *Acc. Chem. Res.* **2004,** *38*, 349-358. (e) Chandler, D., *Nature* **2005,** *437*, 640-647. (f) Rodriguez-Docampo, Z.; Pascu, S. I.; Kubik, S.; Otto, S., *J. Am. Chem. Soc.* **2006,** *128*, 11206-11210. (g) Ma, C. D.; Wang, C.; Acevedo-Velez, C.; Gellman, S. H.; Abbott, N. L., *Nature* **2015,** *517*, 347-350.
(5) Awino, J. K.; Zhao, Y., *J. Am. Chem. Soc.* **2013,** *135*, 12552-12555.
(6) Awino, J. K.; Zhao, Y., *ACS Biomater. Sci. Eng.* **2015,** *1*, 425-430.
(7) (a) Awino, J. K.; Gunasekara, R. W.; Zhao, Y., *J. Am. Chem. Soc.* **2016,** *138*, 9759-9762. (b) Gunasekara, R. W.; Zhao, Y., *J. Am. Chem. Soc.* **2017,** *139*, 829-835.
(8) Zhang, S.; Zhao, Y., *Macromolecules* **2010,** *43*, 4020-4022.
(9) Schmidtchen, F. P., Isothermal Titration Calorimetry in Supramolecular Chemistry. In *Supramolecular Chemistry: From Molecules to Nanomaterials*, Steed, J. W.; Gale, P. A., Eds. Wiley: Online, 2012.
(10) (a) Leo, A.; Hansch, C.; Elkins, D., *Chem. Rev.* **1971,** *71*, 525-616. (b) Sangster, J., *Octanol-Water Partition Coefficients : Fundamentals and Physical Chemistry*. Wiley: Chichester ; New York, 1997; p viii, 170 p.
(11) National Center for Biotechnology Information. PubChem Compound Database; CID=9016 for p-dimethoxybenzene; CID=7731 for p-methylanisole; CID=7809 for p-xylene; CID=7452 for m-dinitrobenzene. https://pubchem.ncbi.nlm.nih.gov/ (accessed Feb 2017).
(12) (a) Smithrud, D. B.; Diederich, F., *J. Am. Chem. Soc.* **1990,** *112*, 339-343. (b) Cubberley, M. S.; Iverson, B. L., *J. Am. Chem. Soc.* **2001,** *123*, 7560-7563. (c) Schneider, H. J., *Angew. Chem. Int. Ed.* **2009,** *48*, 3924-3977.
(13) (a) Hunter, C. A.; Lawson, K. R.; Perkins, J.; Urch, C. J., *J. Chem. Soc. Perkin Trans. 2* **2001**, 651-669. (b) Waters, M. L., *Curr. Opin. Chem. Biol.* **2002,** *6*, 736-741. (c) Scott Lokey, R.; Iverson, B. L., *Nature* **1995,** *375*, 303-305. (d) Gabriel, G. J.; Sorey, S.; Iverson, B. L., *J. Am. Chem. Soc.* **2005,** *127*, 2637-2640.
(14) Hunter, C. A.; Sanders, J. K. M., *J. Am. Chem. Soc.* **1990,** *112*, 5525-5534.
(15) (a) Gago, F., *Methods* **1998,** *14*, 277-292. (b) Ren, J.; Jenkins, T. C.; Chaires, J. B., *Biochemistry* **2000,** *39*, 8439-8447.
(16) If this indeed were the case, the repulsion between the two aromatic rings in compound **5** might not be enough to overcome the hydrophobic interactions, as compound **5** displayed a different energetic profile.